

# Polymeric Films with Three Different Uniplanar Crystalline Phase Orientations

Paola Rizzo, Anna Spatola, Anna De Girolamo Del Mauro, and Gaetano Guerra\*

Dipartimento di Chimica, Università degli Studi di Salerno, Via S. Allende, 84081 Baronissi (Salerno), Italy

Received June 14, 2005; Revised Manuscript Received September 23, 2005

**ABSTRACT:** Semicrystalline syndiotactic polystyrene (s-PS) films, for all crystalline phases based on helical chains ( $\delta$ ,  $\gamma$  and clathrates), have been prepared with high degrees of three different kinds of uniplanar orientation. In particular, by suitable solution- or solvent-induced crystallizations, (010), (002), or (210) crystalline planes of the nanoporous  $\delta$  and clathrate phases can be oriented preferentially parallel to the film plane. To our knowledge, the achievement for a given polymeric crystalline phase of high degrees of three different uniplanar orientations is unprecedented. This is particularly relevant for s-PS due to the functional properties of its nanoporous crystalline  $\delta$  phase as well as of its clathrate phases. As for the clathrate phases, it is also worth noting that, since each cavity of the clathrate phase generally includes one isolated guest molecule whose mobility is generally low, the control of the orientation of the host crystalline phase also allows the control of the orientation of the guest molecules.

## Introduction

The properties of polymeric films depend to a large extent on the kind of orientation built into the structure during processing.<sup>1</sup> As for the crystalline phase orientation of linear polymers, since intrachain covalent bonds are stronger than interchain interactions, the primary slip direction generally is along the chain axes. Hence, as a consequence of uniaxial stretching a *c*-slip mechanism generally occurs, leading to the typical axial orientation. For biaxial stretching, besides the slip direction, also a primary slip plane generally determines the final crystal texture. In fact, a primary slip plane tends to become parallel to the film surface, thus generating the so-called uniplanar (for which a particular molecular or crystal plane tends to be parallel to the film plane) and uniplanar-axial orientations (for which also a particular molecular or crystal axis, generally the chain axis, tends to be parallel to a reference axis).<sup>2</sup> These uniplanar and uniplanar-axial orientations can be achieved for semicrystalline polymers also by other film production procedures, like rolling, solution casting, etc.

For polymers with intermolecular hydrogen bonding, like polyamides, the hydrogen-bonding planes (amide group planes and zigzag methylene sequence planes) tend to be aligned parallel to the surface.<sup>3</sup> For polymers with no specific intermolecular interactions, molecular shape and packing density play major roles in determining the slip planes. For instance, for poly(ethylene terephthalate) the phenyl rings tend to be parallel to the film plane.<sup>2,3a,4</sup> For hydrocarbon polymers, for which the only interchain interactions are of van der Waals type, the primary slip plane generally is that one containing the chain axis and having the highest density. Thus, for instance, it is well established that for the monoclinic  $\alpha$  form of isotactic polypropylene (i-PP) the primary slip plane is the highest density (040) plane, that is, the plane defined by the crystallographic *a* and *c* axes.<sup>5</sup> It is worth noting that often it has been observed the occurrence in a given film of crystallites with different

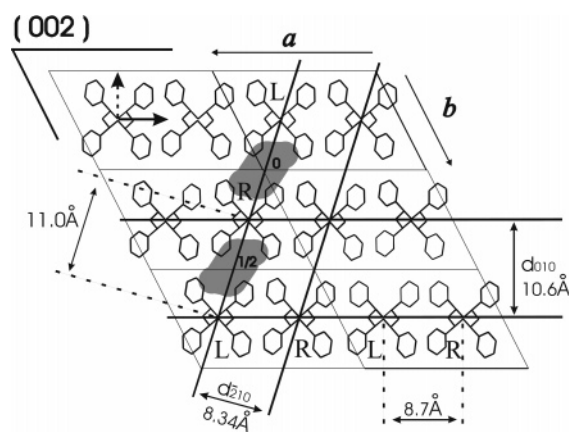


**Figure 1.** Along the chain projection of six adjacent  $\delta$  form unit cells showing traces of the crystalline planes (010) and (210), being perpendicular to the figure, and (002), being parallel to the figure, which can be preferentially aligned parallel to the film plane. Two crystalline cavities (gray regions) are labeled by approximate *z* fractional coordinates of their barycenters. The interchain distances for the (010) and (210) crystalline plane, as well as their interplanar distances ( $d_{010}$  and  $d_{210}$ ), are explicitly indicated. Both (010) and (210) planes are characterized by successions of anticlinical helices.

kinds of uniplanar orientation. For instance, some i-PP films beside the uniplanar orientation relative to the (040) plane can present also minor uniplanar orientations involving the (110) and (130) planes.<sup>5b–d</sup>

As for clathrate phases<sup>6</sup> and the nanoporous  $\delta$  phase<sup>7</sup> of syndiotactic polystyrene (s-PS), high degrees of (010) uniplanar orientation ( $f_{010} \geq 0.75$ ) can be easily achieved by solvent treatments of biaxially stretched amorphous films<sup>8a</sup> as well as, without any stretching, by solution-casting procedures.<sup>8b</sup> This kind of uniplanar orientation can be easily rationalized<sup>8</sup> since the (010) planes present a maximum interplanar distance and correspond to rows of parallel helices with minimum interchain distance.<sup>6,7</sup> For instance, for the empty  $\delta$  phase (monoclinic with  $a = 17.4$  Å,  $b = 11.85$  Å,  $c = 7.7$  Å,  $\gamma = 117^\circ$ ; see along the chain projection of Figure 1),<sup>7</sup> the interplanar ( $d_{010} = \lambda/(2 \sin \theta_{010})$ ) and the interchain distances are 10.6 and 8.7 Å, respectively.

\* Corresponding author: e-mail gguerra@unisa.it.

Recently, again for s-PS  $\delta$  and clathrate phases, a different kind of orientation presenting the crystalline chain axes nearly perpendicular to the film plane has been achieved, by casting procedures with different solvents<sup>9a</sup> as well as by guest-induced crystallization of unstretched amorphous films.<sup>9b</sup> This kind of orientation can also be defined as uniplanar orientation as for the (002) plane, since this plane which is normal to the chain axes (i.e., parallel to the projection of Figure 1) tends to be parallel to the film plane. Also for this kind of uniplanar orientation high degrees ( $f_{002}$  up to 0.75) can be easily achieved.

It has also been established that both kinds of uniplanar orientations can be maintained<sup>8b,9b</sup> after thermal treatments,<sup>10</sup> leading to the formation of the dense  $\gamma$  phase,<sup>10b</sup> i.e., of the other crystalline phase presenting s(2/1)2 helices.

In this paper we show that, for all helical crystalline phases of s-PS ( $\delta$ ,  $\gamma$ , and clathrates) by suitable processing, it is possible to achieve films with high degrees of a third new kind of uniplanar orientation.

### Experimental Part

The s-PS used in this study was manufactured by Dow Chemical Co. under the trademark Questa 101. The <sup>13</sup>C nuclear magnetic resonance characterization showed that the content of syndiotactic triads was over 98%. The weight-average molar mass obtained by gel permeation chromatography (GPC) in trichlorobenzene at 135 °C was found to be  $M_w = 3.2 \times 10^5$  with the polydispersity index  $M_w/M_n = 3.9$ .

Films with (010) and (002) uniplanar orientations have been obtained by solution-casting procedures at room temperature from 0.5 wt % s-PS solutions in chloroform and trichloroethylene, respectively. Films with ( $\bar{2}10$ ) uniplanar orientation have been obtained by immersion of an amorphous 50  $\mu\text{m}$  film at 50 °C for 1 h in *o*-xylene or in 1,4-dimethylnaphthalene. These rigid and transparent films present degrees of crystallinity, obtained by FTIR spectral subtraction procedures,<sup>11</sup> in the range 35–40%.

Wide-angle X-ray diffraction patterns with nickel-filtered Cu K $\alpha$  radiation were obtained, in reflection, with an automatic Philips powder diffractometer as well as, in transmission, by using a cylindrical camera (radius = 57.3 mm). In the latter case the patterns were recorded on a BAS-MS imaging plate (FUJIFILM) and processed with a digital imaging reader (FUJIBAS 1800).

In particular, to recognize the kind of crystalline orientation present in the samples, photographic X-ray diffraction patterns were taken by placing the film sample parallel to the axis of the cylindrical camera and by sending the X-ray beam parallel or perpendicular to the film surface, as shown on the left of Figure 3, A and B, respectively.

The degree of the different kinds of uniplanar orientation of the crystallites with respect to the film plane has been formalized on a quantitative numerical basis using Hermans' orientation functions, in analogy to that one defined for the axial orientation in ref 12:

$$f_{hkl} = (3 \overline{\cos^2 \chi_{hkl}} - 1)/2 \quad (1)$$

by assuming  $\overline{\cos^2 \chi_{hkl}}$  as the squared average cosine value of the angle,  $\chi_{hkl}$ , between the normal to the film surface and the normal to the ( $hkl$ ) crystallographic plane.

Since, in our cases, a  $\theta_{hkl}$  incidence of X-ray beam is used, the quantity  $\overline{\cos^2 \chi_{hkl}}$  can be easily experimentally evaluated:

$$\overline{\cos^2 \chi_{hkl}} = \overline{\cos^2 \chi_{hkl}} = \frac{\int_0^{\pi/2} I(\chi_{hkl}) \cos^2 \chi_{hkl} \sin \chi_{hkl} d\chi_{hkl}}{\int_0^{\pi/2} I(\chi_{hkl}) \sin \chi_{hkl} d\chi_{hkl}} \quad (2)$$

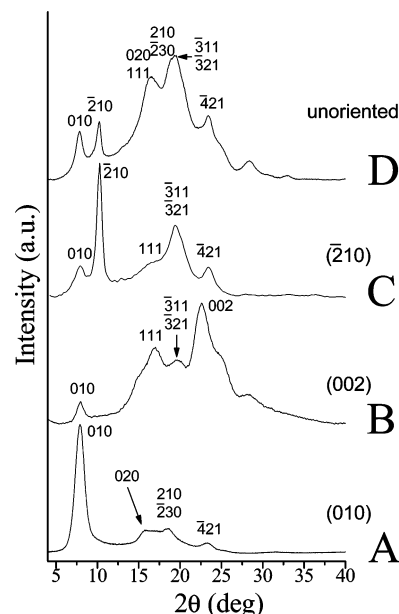


**Figure 2.** X-ray diffraction patterns (Cu K $\alpha$ ), obtained by an automatic powder diffractometer, of samples including 8–10 wt % of *o*-xylene and presenting different uniplanar orientations of the s-PS/*o*-xylene clathrate phase. The samples have been obtained by *o*-xylene treatments of (A) film cast from chloroform, (B) film cast from trichloroethylene, (C) amorphous film, and (D)  $\delta$  form powder. The Miller indexes of relevant reflections are indicated near the peaks.

where  $I(\chi_{hkl})$  is the intensity distribution of a ( $hkl$ ) diffraction on the Debye ring and  $\chi_{hkl}$  is the azimuthal angle measured from the equator.

The diffracted intensities  $I(\chi_{hkl})$  of eq 2 were obtained by using an AFC7S Rigaku automatic diffractometer (with a monochromatic Cu K $\alpha$  radiation) and were collected sending the X-ray beam parallel to the film surface and maintaining an equatorial geometry. Because the collection was performed at constant  $2\theta$  values and in the equatorial geometry, the Lorenz and polarization corrections were unnecessary.

In these assumptions,  $f_{hkl}$  is equal to 1 and  $-0.5$  if ( $hkl$ ) planes of all crystallites are perfectly parallel and perpendicular to the plane of the film, respectively.

Infrared spectra were obtained at a resolution of 1.0  $\text{cm}^{-1}$  with a Vector 22 Bruker spectrometer equipped with deuterated triglycine sulfate (DTGS) detector and a Ge/KBr beam splitter. The frequency scale was internally calibrated to 0.01  $\text{cm}^{-1}$  using a He–Ne laser. 32 scans were signal-averaged to reduce the noise.

### Results and Discussion

X-ray diffraction patterns, collected by an automatic powder diffractometer, of different s-PS/*o*-xylene clathrate samples, having a thickness of 40–50  $\mu\text{m}$  and including 8–10 wt % of *o*-xylene, have been reported in Figure 2. In particular, the patterns of Figure 2A,B refer to films with (010) and (002) uniplanar orientations, obtained by *o*-xylene treatment of s-PS clathrate films cast from chloroform and from trichloroethylene, respectively. It is worth noting that although the initial guest molecules (chloroform and trichloroethylene) have been fully replaced by the new guest (*o*-xylene), as shown by FTIR measurements (not reported), the X-ray diffraction patterns of Figure 2A,B are similar to those of the starting cast films and show high intensity of the (010) and (002) reflections, respectively.

The X-ray diffraction pattern of a clathrate s-PS/*o*-xylene film obtained by immersion at 50 °C for 1 h in *o*-xylene of an amorphous 50  $\mu\text{m}$  film is shown in Figure

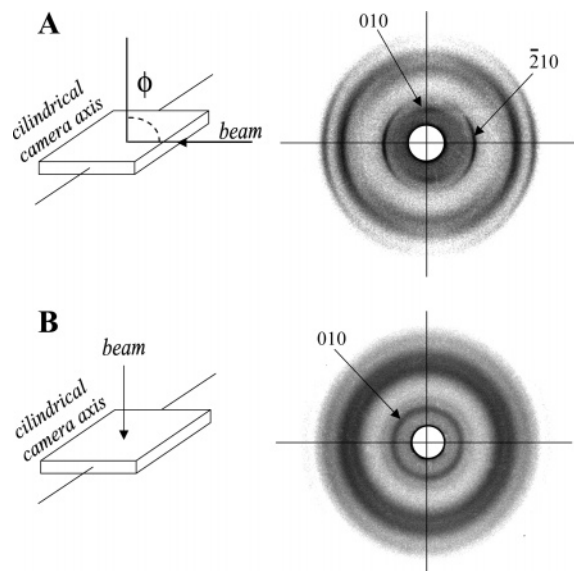


**Figure 3.** X-ray diffraction patterns taken with beam parallel (A) and perpendicular (B) to the film plane, for the film presenting the s-PS/*o*-xylene clathrate phase with a  $(\bar{2}10)$  uniplanar orientation of Figure 2C.

2C. For the sake of comparison, the X-ray diffraction pattern of a semicrystalline powder (obtained by *o*-xylene treatment of an unoriented  $\delta$  form powder) presenting the unoriented s-PS/*o*-xylene clathrate phase is also shown in Figure 2D. The peaks of all diffraction patterns of Figure 2A–D can be indexed by a monoclinic unit cell similar to that one reported for the s-PS clathrate form, including *o*-dichlorobenzene ( $a = 17.5$  Å,  $b = 14.4$  Å,  $c = 7.8$  Å, and  $\gamma = 127.4^\circ$ ),<sup>6f</sup> i.e., a guest isosteric with *o*-xylene.

Substantial differences between the relative intensities of the reflections, for the profiles of Figure 2, clearly indicate the occurrence for the film of Figure 2C of a new kind of orientation. In particular, the most intense reflection (at  $2\theta_{Cu K\alpha} = 10.2^\circ$ ) is indexed as  $(\bar{2}10)$ , thus suggesting a preferential parallel orientation of this crystalline plane with respect to the film plane.

A better understanding of the crystalline phase orientation of the film of Figure 2C can be achieved by the X-ray diffraction patterns taken with beam parallel and perpendicular to the film plane and collected on a photographic cylindrical camera, which are shown in Figure 3, A and B, respectively. The pattern B presents only Debye rings while the pattern A presents intense  $(\bar{2}10)$  reflection arcs centered on the equatorial line and weak nearly meridional  $(010)$  reflection arcs. These data again suggest the occurrence of the  $(\bar{2}10)$  uniplanar orientation.

The occurrence of the  $(\bar{2}10)$  uniplanar orientation for this s-PS film has been further confirmed by the plot of the intensity of the  $(\bar{2}10)$  reflection vs the orientation angle  $\phi$ , between the X-ray beam and the normal to the film plane (Figure 4). In fact,  $I(\bar{2}10)$  presents a broad maximum for X-ray beam parallel to the film plane ( $\phi \approx 90^\circ$ , Figure 3A), which is compatible with the superposition of two broad maxima centered at  $90^\circ \pm \theta$  (i.e.,  $84.9^\circ$  and  $95.1^\circ$ ) as expected for  $(\bar{2}10)$  planes preferentially parallel to the film plane.

For the uniplanar oriented clathrate films, whose X-ray diffraction patterns are reported in Figure 2A–C, the orientation factor of the  $(010)$ ,  $(002)$ , and  $(\bar{2}10)$  crystallographic planes, as evaluated on the basis of the

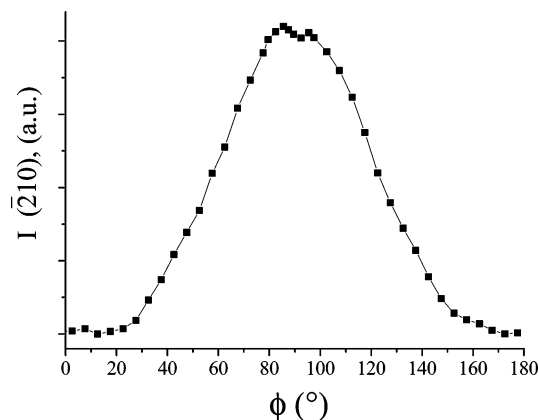


**Figure 4.** Intensity of the  $(\bar{2}10)$  reflection, collected at  $2\theta = 10.2^\circ$ , and reported versus the film rotation angle  $\phi$ , between the X-ray beam and the normal to the film plane (Figure 3A), for the film of Figure 2C presenting the s-PS/*o*-xylene clathrate phase.

intensity distribution of the corresponding reflections (by eqs 1 and 2) has been evaluated as  $f_{010} = 0.75$ ,  $f_{002} = 0.7$ , and  $f_{\bar{2}10} = 0.6$ , respectively.

The occurrence of this new kind of uniplanar orientation can be rationalized by considering that the  $(\bar{2}10)$  crystallographic plane is a suitable slip plane. In fact, it contains the chain axis, and it has, by excluding the  $(010)$  plane, maximum interplanar distance and minimum interchain distance. For instance, for the empty  $\delta$  phase<sup>7</sup> (Figure 1), the interplanar ( $d_{\bar{2}10} = \lambda/(2 \sin \theta_{\bar{2}10})$ ) and the interchain distances are 8.34 and 11.0 Å, respectively. As can be seen already on inspection of Figure 1, due to the inclusion of suitable guest molecules,  $(\bar{2}10)$  planes can achieve a planar density comparable with that one of the  $(010)$  planes, and hence they can become primary slip planes. It is also worth adding that both  $(010)$  and  $(\bar{2}10)$  planes are characterized by successions of adjacent anticlinal helices.

This new kind of uniplanar orientation can be also more efficiently achieved by treatment of amorphous s-PS films by an other bulky planar guest (1,4-dimethylnaphthalene, thereafter DMNP), as shown for instance by the X-ray diffraction pattern (taken with an automatic powder diffractometer) of an amorphous 50  $\mu\text{m}$  film after immersion at 50  $^\circ\text{C}$  for 1 h (Figure 5A). The pattern of Figure 5A, beside the intense  $(\bar{2}10)$  reflection, also presents the second order of this reflection ( $420$  at  $2\theta_{Cu K\alpha} = 20.3^\circ$ ) and the degree of uniplanar orientation is high ( $f_{\bar{2}10} = 0.7$ ). It is worth adding that X-ray diffraction patterns taken with the beam perpendicular to the film (like that one of Figure 3B) show the  $(010)$  diffraction peak at a very low angle ( $2\theta_{Cu K\alpha} \approx 5.7^\circ$ ), corresponding to a large Bragg spacing ( $d_{010} \approx 1.55$  nm). This value, also larger than that one observed for the s-PS/norbornadiene intercalate phase ( $d_{010} \approx 1.35$  nm),<sup>13</sup> suggests that also the s-PS/DMNP molecular complex phase could be constituted by layers of enantiomorphous polymer  $s(2/1)2$  helices intercalated by layers of guest molecules.

X-ray diffraction patterns of  $\delta$  and  $\gamma$  semicrystalline films, obtained from the s-PS/DMNP molecular complex film of Figure 5A, after guest extraction by carbon dioxide<sup>7b</sup> and after annealing at 160  $^\circ\text{C}$ ,<sup>10</sup> are reported in Figure 5, B and C, respectively.

The maintenance of the  $(\bar{2}10)$  orientation in the  $\delta$  phase (Figure 5B) is clearly shown by the high intensity of the  $(\bar{2}10)$  reflection, which is very weak for the  $\delta$  form



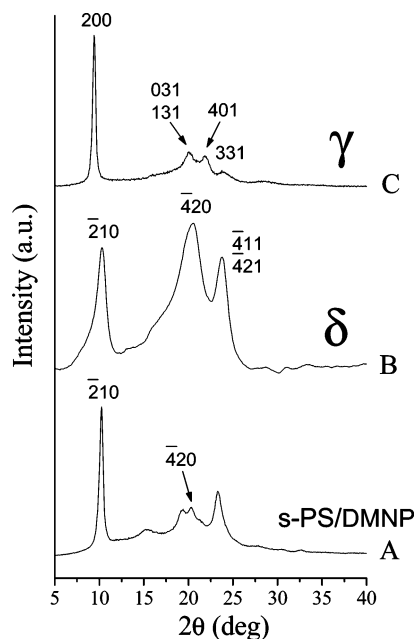


**Figure 5.** X-ray diffraction patterns, obtained by an automatic powder diffractometer, of s-PS semicrystalline films: (A) obtained by immersion of an amorphous film in DMNP (s-PS/DMNP molecular-complex phase); (B) the film of (A) after guest extraction by carbon dioxide (nanoporous  $\delta$  phase); (C) the film of (A) after annealing at 160 °C ( $\gamma$  phase). The diffraction peaks of the  $\delta$  and  $\gamma$  phases have been indexed by the monoclinic and orthorhombic unit cells described in refs 7a and 10b, respectively.

and not detectable by X-ray diffraction patterns of unoriented powders or of films with (010) or (002) uniplanar orientations (as shown by Figure 6 of ref 8b). It is worth noting that although the spectrum of the  $\delta$  form film (Figure 5B), when compared with the molecular complex pattern (Figure 5A), presents a reduced intensity of the (210) reflection, the evaluated degree of uniplanar orientation remains nearly unaltered ( $f_{210} = 0.7$ ).

The X-ray diffraction pattern of the  $\gamma$  semicrystalline film (Figure 5C), obtained from the s-PS/DMNP molecular complex film with (210) uniplanar orientation, shows a very intense reflection at  $2\theta_{Cu K\alpha} = 9.3^\circ$ , which can be indexed as (200), on the basis of the orthorhombic unit cell.<sup>10b</sup> This reflection is only of medium intensity for  $\gamma$  form unoriented samples and not detectable by X-ray diffraction patterns of films with (010) or (002) uniplanar orientations (as shown by Figure 3 of ref 8b). Hence, as a consequence of the thermal annealing, the (210) crystalline planes of  $\delta$  and clathrate phases are transformed into (200) crystalline planes of the  $\gamma$  phase, while the degree of orientation is essentially maintained. It is worth noting, incidentally, that this result can contribute to the definition of the crystalline structure of the  $\gamma$  phase, which is still unknown, starting from the known crystalline structure of the  $\delta$  phase.<sup>7a</sup>

The control of crystalline phase orientation for s-PS could be relevant for its structural and functional properties. Just as a preliminary example, infrared absorbance spectra of s-PS films presenting the nanoporous crystalline  $\delta$  phase with the three different kinds of uniplanar orientations have been compared in Figure 6. It is apparent that the occurrence of the uniplanar orientations heavily affects the intensity of peaks of the helical crystalline host phase,<sup>14</sup> labeled by  $\perp$  or  $\parallel$  in Figure 6, depending on the direction of their transition

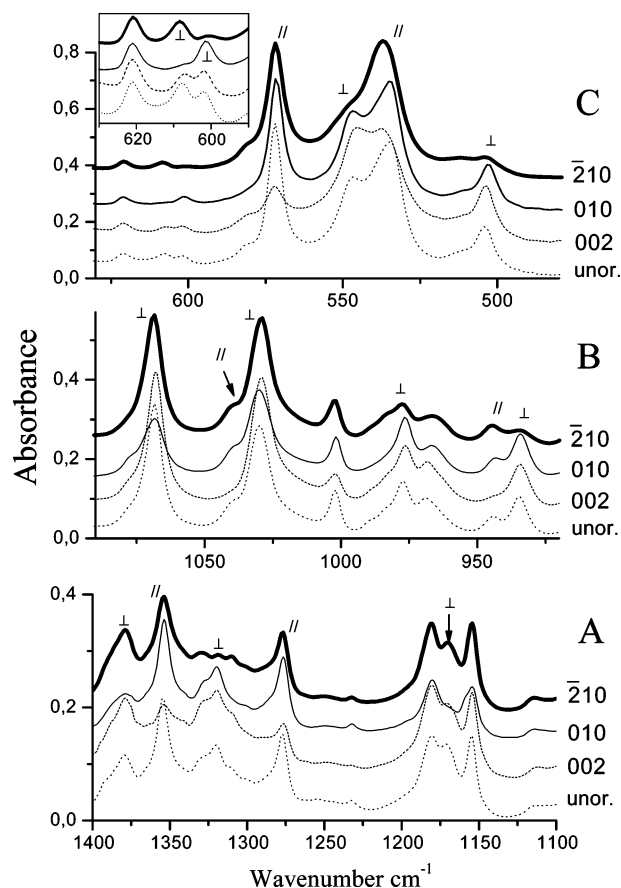


**Figure 6.** FTIR spectra in the wavenumber ranges 1400–1100  $\text{cm}^{-1}$  (A), 1080–925  $\text{cm}^{-1}$  (B), and 630–480  $\text{cm}^{-1}$  (C), of  $\delta$  form films: (···) unoriented; with (---) (002), (—) (010), and (—) (210) uniplanar orientation. Peaks corresponding to the host helical crystalline phase of s-PS are labeled by  $\perp$  and  $\parallel$ , depending on the direction of their transition moment vectors nearly perpendicular or parallel to the chain axis (based on independent measurements on uniaxially stretched films).

moment vectors, perpendicular or parallel to the chain axis (as established by infrared linear dichroism analysis on uniaxially stretched s-PS clathrate films).<sup>15</sup>

As expected, all peaks corresponding to vibrational modes whose transition moment vectors are parallel to the chain axis (e.g., at 1354, 1278, 1039, 941, 769, 571, 538  $\text{cm}^{-1}$ ) are of high intensity for the spectra of films with (010) and (210) uniplanar orientations (continuous lines in Figure 6) and of low intensity for the spectra of films with (002) orientation (dashed line in Figure 6). More informative are the peaks corresponding to vibrational modes whose transition moment vectors are perpendicular to the chain axis and hence of high intensity for films with (002) orientation. In fact, some of them (1320, 976, 934, 602, 548, 505  $\text{cm}^{-1}$ ) are of high intensity for films with (010) orientation, and hence their transition moment vectors are roughly along the  $\langle 010 \rangle$  direction, i.e., nearly parallel to the 2-fold axis perpendicular to the  $s(2/1)_2$  helix and passing through the external methylenes (see the thick arrow shown for an helix on the left of Figure 1). On the other hand, other “perpendicular” peaks (1169, 1068, 1029, 608  $\text{cm}^{-1}$ ) are of high intensity for films with (210) uniplanar orientation, and hence their transition moment vectors are roughly along the  $\langle 210 \rangle$  direction, i.e., possibly parallel to the 2-fold axis perpendicular to the  $s(2/1)_2$  helix and passing through the inner methylenes (see the

dashed arrow shown for an helix on the left of Figure 1).

## Conclusions

Semicrystalline s-PS films, for all crystalline phases based on helical chains ( $\delta$ ,  $\gamma$ , and clathrates), can be prepared with high degrees of three different kinds of uniplanar orientation. In particular, this paper describes a procedure to obtain a third kind of uniplanar orientation which adds to the already known (010) and (002) uniplanar orientations.

This new kind of uniplanar orientation, involving an orientation of the (210) crystalline planes preferentially parallel to the film plane, can be achieved for *o*-xylene and 1,4-dimethylnaphthalene molecular complex phases obtained by solvent-induced crystallization of amorphous s-PS films. By suitable procedures, starting from these films, the same kind of orientation can be maintained for all molecular complex phases as well as for the nanoporous  $\delta$  phase. Moreover, thermal treatments on these molecular complex and  $\delta$  phases, presenting the (210) uniplanar orientation, lead to a new kind of uniplanar orientation also for the  $\gamma$  phase, corresponding to a preferential orientation of the (200) crystalline planes preferentially parallel to the film plane.

To our knowledge, the achievement of polymeric films presenting a given crystalline phase with high degrees of three different uniplanar orientations is unprecedented. This is particularly relevant for  $\delta$  and molecular complex phases of s-PS due to their functional properties.<sup>16–18</sup>

In particular, as for the nanoporous  $\delta$  phase, due to its use in molecular separations<sup>16</sup> as well as in sensors,<sup>17</sup> a precise control of the crystalline phase orientation should allow a control of diffusivity of the guest molecules. In fact, according to molecular dynamics simulations, the guest diffusivity would be minimum and maximum for directions perpendicular and parallel to the dense crystallographic (010) planes, respectively.<sup>19</sup> This suggests that films with (010) and (210) uniplanar orientations could present minimum and maximum guest diffusivity, respectively.

As for the clathrate phases, it is worth noting that, since each cavity of the clathrate phase generally includes isolated guest molecules whose mobility is generally low,<sup>20</sup> the control of the orientation of the host crystalline phase also allows the control of the orientation of the isolated guest molecules.<sup>15</sup> This gives the opportunity to make spectroscopical characterizations of “isolated” guest molecules, presenting three different and well-defined orientations with respect to the incident radiation beam.

The control of the orientation of molecular complex phases (both clathrate and intercalate) could be relevant for the case of active guests (e.g., fluorescent, photoreactive, chromophore, etc.),<sup>18</sup> since it could allow the control of their functional properties.

**Acknowledgment.** Prof. Attilio Immirzi and Dr. Vincenzo Venditto of University of Salerno and Dr. Pellegrino Musto of the Institute of Research and Technology of Plastic Materials of the National Research Council of Italy are gratefully acknowledged for useful discussions. Financial support from the “Ministero dell’Istruzione, dell’Università e della Ricerca” (PRIN 2004 and FIRB 2001) and from Regione Campania

(Legge 5 and Centro di Competenza) is gratefully acknowledged.

## References and Notes

- (1) (a) Ward, I. M. In *Structures and Properties of Oriented Polymers*; Chapman & Hall: London, 1975; Chapter 1, p 1. (b) Frommer, J. E.; Chance, R. R. In *Encyclopedia of Polymer Science and Engineering*, 2nd ed.; Wiley-Interscience: New York, 1986; Vol. 5, p 462.
- (2) Heffelfinger, C. J.; Burton, R. L. *J. Polym. Sci.* **1960**, *47*, 289.
- (3) (a) Akabane, T.; Mochizuchi, T. *J. Polym. Sci., Polym. Lett.* **1970**, *7*, 487. (b) Penel-Pierron, L.; Seguela, R.; Lefebvre, J.-M.; Miri, V.; Depecker, C.; Jutigny, M.; Pabiot, J. *J. Polym. Sci., Part B: Polym. Phys.* **2001**, *39*, 1224. (c) Rhee, S.; White, J. L. *J. Polym. Sci., Part B: Polym. Phys.* **2002**, *40*, 1189, 2624.
- (4) (a) Werner, E.; Janocha, S.; Hopper, M. J.; Mackenzie *Encyclopedia of Polymer Science and Engineering*, 2nd ed.; Wiley-Interscience: New York, 1986; Vol. 12, p 193. (b) Gohil, R. M. *J. Appl. Polym. Sci.* **1993**, *48*, 1649.
- (5) (a) Sobue, H.; Tabata, J. *J. Appl. Polym. Sci.* **1959**, *2*, 62. (b) Uejo, H.; Hoshino, S. *J. Appl. Polym. Sci.* **1970**, *14*, 317. (c) Bartczak, Z.; Martuscelli, E. *Polymer* **1997**, *38*, 4139. (d) Rizzo, P.; Venditto, V.; Guerra, G.; Vecchione, A. *Macromol. Symp.* **2002**, *185*, 53.
- (6) (a) Chatani, Y.; Shimane, Y.; Inagaki, T.; Ijitsu, T.; Yukinari, T.; Shikuma, H. *Polymer* **1993**, *34*, 1620. (b) Chatani, Y.; Inagaki, T.; Shimane, Y.; Shikuma, H. *Polymer* **1993**, *34*, 4841. (c) De Rosa, C.; Rizzo, P.; Ruiz de Ballesteros, O.; Petraccone, V.; Guerra, G. *Polymer* **1999**, *40*, 2103. (d) Milano, G.; Venditto, V.; Guerra, G.; Cavallo, L.; Ciambelli, P.; Sannino, D. *Chem. Mater.* **2001**, *13*, 1506. (e) Tarallo, O.; Petraccone, V. *Macromol. Chem. Phys.* **2004**, *205*, 1351. (f) Tarallo, O.; Petraccone, V. *Macromol. Chem. Phys.* **2005**, *206*, 672.
- (7) (a) De Rosa, C.; Guerra, G.; Petraccone, V.; Pirozzi, B. *Macromolecules* **1997**, *30*, 4147. (b) Reverchon, E.; Guerra, G.; Venditto, V. *J. Appl. Polym. Sci.* **1999**, *74*, 2077.
- (8) (a) Rizzo, P.; Albuñia, A. R.; Milano, G.; Venditto, V.; Guerra, G.; Mensitieri, G.; Di Maio, L. *Macromol. Symp.* **2002**, *185*, 65. (b) Rizzo, P.; Lamberti, M.; Albuñia, A. R.; Ruiz de Ballesteros, O.; Guerra, G. *Macromolecules* **2002**, *35*, 5854.
- (9) (a) Rizzo, P.; Costabile, A.; Guerra, G. *Macromolecules* **2004**, *37*, 3071. (b) Rizzo, P.; Della Guardia, S.; Guerra, G. *Macromolecules* **2004**, *37*, 8043.
- (10) (a) Guerra, G.; Vitagliano, V. M.; De Rosa, C.; Petraccone, V.; Corradini, P. *Macromolecules* **1990**, *23*, 1539. (b) As for the  $\gamma$  phase, an orthorhombic unit cell with  $a = 19.15$  Å,  $b = 17.0$  Å, and  $c = 7.7$  Å has been derived by electron diffraction measurements on single crystals (Ruiz de Ballesteros, O., unpublished data) and confirmed by X-ray diffraction patterns of films with (010)<sup>8b</sup> and (002)<sup>9b</sup> uniplanar orientations.
- (11) (a) Albuñia, A. R.; Musto, P.; Guerra, G. *Polymer*, in press. (b) Daniel, C.; Guerra, G.; Musto, P. *Macromolecules* **2002**, *35*, 2243.
- (12) (a) Samuels, R. J. In *Structured Polymer Properties*; John Wiley & Sons: New York, 1971; Chapter 2, p 28. (b) Kakudo, M.; Kasai, N. *X-Ray Diffraction by Polymers*; Elsevier: Amsterdam, 1972; Chapter 10, p 252. (c) Alexander, L. E. In *X-ray Diffraction Methods in Polymer Science*; Krieger, R. E., Ed.; Huntington: New York, 1979; Chapter 4, p 210.
- (13) Petraccone, V.; Tarallo, O.; Venditto, V.; Guerra, G. *Macromolecules* **2005**, *38*, 6965.
- (14) (a) Reynolds, N. M.; Savage, J. D.; Hsu, S. L. *Macromolecules* **1989**, *22*, 2869. (b) Guerra, G.; Musto, P.; Karasz, F. E.; Macknight, W. J. *Makromol. Chem.* **1990**, *191*, 2111. (c) Vittoria, V. *Polym. Commun.* **1990**, *31*, 263. (d) Reynolds, N. M.; Stidham, J. D.; Hsu, S. L. *Macromolecules* **1991**, *24*, 3662. (e) Tashiro, K.; Ueno, Y.; Yoshioka, A.; Kobayashi, M. *Macromolecules* **2001**, *34*, 310. (f) Yoshioka, A.; Tashiro, K. *Macromolecules* **2003**, *36*, 3001.
- (15) Albuñia, R. A.; Di Masi, S.; Rizzo, P.; Milano, G.; Musto, P.; Guerra, G. *Macromolecules* **2003**, *36*, 8695.
- (16) (a) Manfredi, C.; Del Nobile, M. A.; Mensitieri, G.; Guerra, G.; Rapacciuolo, M. *J. Polym. Sci., Polym. Phys. Ed.* **1997**, *35*, 133. (b) Guerra, G.; Manfredi, C.; Musto, P.; Tavone, S. *Macromolecules* **1998**, *31*, 1329. (c) Guerra, G.; Milano, G.; Venditto, V.; Musto, P.; De Rosa, C.; Cavallo, L. *Chem. Mater.* **2000**, *12*, 363. (d) Musto, P.; Mensitieri, G.; Cotugno, S.; Guerra, G.; Venditto, V. *Macromolecules* **2002**, *35*, 2296. (e) Sivakumar, M.; Yamamoto, Y.; Amutharani, D.; Tsujita, Y.; Yoshimizu, H.; Kinoshita, T. *Macromol. Rapid Commun.* **2002**, *23*, 77. (f) Saitoh, A.; Amutharani, D.; Yamamoto, Y.;

- Tsujita, Y.; Yoshimizu, H. *Desalination* **2002**, *148*, 353. (g) Yamamoto, Y.; Kishi, M.; Amutharani, D.; Sivakumar, M.; Tsujita, Y.; Yoshimizu, H. *Polym. J.* **2003**, *35*, 465. (h) Saitoh, A.; Amutharani, D.; Yamamoto, Y.; Tsujita, Y.; Yoshimizu, H.; Okamoto, S. *Polym. J.* **2003**, *35*, 868. (i) Tamai, Y.; Fukuda, M. *Chem. Phys. Lett.* **2003**, *371*, 620. (j) Daniel, C.; Alfano, D.; Venditto, V.; Cardea, S.; Reverchon, E.; Larobina, D.; Mensitieri, G.; Guerra, G. *Adv. Mater.* **2005**, *17*, 1515.
- (17) (a) Mensitieri, G.; Venditto, V.; Guerra, G. *Sens. Actuators, B* **2003**, *92*, 255. (b) Giordano, M.; Russo, M.; Cusano, A.; Cutolo, A.; Mensitieri, G.; Nicolais, L. *Appl. Phys. Lett.* **2004**, *85*, 22. (c) Giordano, M.; Russo, M.; Cusano, A.; Mensitieri, G.; Guerra, G. *Sens. Actuators, B* **2005**, *109*, 177.
- (18) (a) Venditto, V.; Milano, G.; De Girolamo Del Mauro, A.; Guerra, G.; Mochizuki, J.; Itagaki, H. *Macromolecules* **2005**, *38*, 3696. (b) Stegmaier, P.; De Girolamo Del Mauro, A.; Venditto, V.; Guerra, G. *Adv. Mater.* **2005**, *17*, 1166. (c) Uda, Y.; Kaneko, F.; Tanigaki, N.; Kawaguchi, T. *Adv. Mater.* **2005**, *17*, 1846.
- (19) Milano, G.; Guerra, G.; Müller-Plathe, F. *Chem. Mater.* **2002**, *14*, 2977.
- (20) (a) Trezza, E.; Grassi, A. *Macromol. Rapid Commun.* **2002**, *23*, 260. (b) Alburnia, A. R.; Graf, R.; Guerra, G.; Spiess, H. W. *Macromol. Chem. Phys.* **2005**, *206*, 715–724.

MA051247P